Available online at www.sciencedirect.com

ScienceDirect

Procedia IUTAM 20 (2017) 34 – 41

Procedia IUTAM

www.elsevier.com/locate/procedia

24th International Congress of Theoretical and Applied Mechanics

Comparing nonlinear free vibrations of Timoshenko beams with mechanical or geometric curvature definition

Stefano Lenci[a,*], Francesco Clementi[a], Giuseppe Rega[b]

[a]*DICEA, Polytechnic University of Marche, via Brecce Bianche 12, Ancona 60131, Italy*
[b]*DISG, Sapienza University of Rome, via A. Gramsci 53, Rome 00197, Italy*

Abstract

The nonlinear free oscillations of a planar, initially straight Timoshenko beam are investigated by means of the asymptotic development method. Attention is focus on the difference in considering the "mechanical" vs the "geometric" curvature of the axis of the beam, which are different for extensible beams. A comparison of the results obtained by the two models is proposed, and it is shown when they are equivalent and when they give different nonlinear behaviours. A parametric analysis showing the effects of the slenderness (arbitrary, not necessarily large) and of the stiffness of the right-end axial spring is performed.

Peer-review under responsibility of organizing committee of the 24th International Congress of Theoretical and Applied Mechanics

Keywords: Timoshenko beam; Curvature definition; Arbitrary slenderness; Axial spring; Nonlinear free oscillations; Asymptotic solution.

1. Introduction

Beam models can be obtained by two different approaches. In the first, named "three dimensional approach"[1] or "induced theories"[2], the equations are derived from a fully 3D "parent" problem, by means of some appropriate mathematical techniques, like for example asymptotic methods[3,4] or internal constraints[5], taking into account the specific geometrical (and mechanical) properties, in particular its cylindrical-like shape. The second approach, named "direct approach"[1] or "intrinsic theories"[2], consists of regarding the system directly as a 1D continuum, with its own mechanical properties and related descriptors. Here the 3D nature of the body is somehow hidden, as it appears only in the definition of the parameters entering the equations, and one makes assumptions directly on the beam axis.

The two approaches are alternative, being more rigorous but more demanding and somehow more "rigid" the former, more immediate and thus easier and more "open" the latter.

The difference relies in the level at which one introduces the hypothesis necessary to end up with the beam equations. In the first approach this is mainly done in the "reduction" process, where one makes some assumption on the behaviour of the 3D displacements, on smallness of some parameters (e.g. the cross-section dimensions), etc. In the second approach this is commonly done in choosing the kinematic descriptors (i.e. strain measures), and the constitutive behaviour, which are the *main* assumptions calling for a detailed investigation.

* Corresponding author. Tel.: +39-071-220-4552 ; fax: +39-071-220-4576.
E-mail address: lenci@univpm.it

Peer-review under responsibility of organizing committee of the 24th International Congress of Theoretical and Applied Mechanics
doi:10.1016/j.piutam.2017.03.006

Limiting to the case of flexural behaviour, it is accepted that the bending moment is a (possibly nonlinear) function of the curvature of the beam axis [1,6], $M = M(k)$. However, two conceptually different curvatures can be defined,

$$k_m = \frac{d\theta}{dZ}, \qquad \text{or} \qquad k_g = \frac{d\theta}{dS} = \frac{d\theta}{dZ}\frac{dZ}{dS} = \frac{k_m}{1+e}, \tag{1}$$

where θ is the rotation of the beam cross-section (which corresponds to the deflection angle of the beam axis for Euler-Bernoulli beams, and which is instead an intrinsic variable for Timoshenko beams), dZ and dS are the length of the *undeformed* and *deformed* beam element, respectively, and $e = \frac{dS}{dZ} - 1$ is the elongation of the beam axis [7]. Clearly, the difference appears only for *extensible* beams, for which $e \neq 0$. Furthermore, we note that in the linear case $e << 1$, so that the two definitions are identical, and the difference is relevant only in the *nonlinear* regime.

We name the former "normalized", "flexural" or "mechanical" curvature [6,8,9], and the latter "geometric" curvature [8,10]. Note that the normalized curvature is defined as the material measure of curvature [11,12] and the geometric curvature is denoted as the spatial measure of curvature [10,12].

Now the question arises of which is the "proper" curvature [13]. Actually, in the literature k_m is commonly used [2,6,9,10,14], with various motivations: its simplicity, its capability to isolate the effect of pure bending from curvature variations produced by stretching, etc. However, at least in [6,7,8,12,15,16,17,18] k_g is used (or at least addressed), mainly because it is considered to be the more correct curvature due to its geometric meaning.

It must be remarked that, since the choice of the curvature is an assumption, thus being part of the model, both expressions (1) are correct in principle within the direct or intrinsic approach. Preferring one with respect to the other is only related to the predictive capability of the ensuing model, and thus the choice should be made by comparing the results of the model with other independent results: experimental, numerical or theoretical (i.e., comparing with the constitutive equation coming from 3D or induced theories).

It will not be very surprising to *not* get to a unique answer, being one model preferable in some circumstances and the other better in different cases. Thus, it is interesting to ascertain the differences obtained by considering the two models, to be used for comparison purposes in further developments. This is the goal of this work, which adds to other previous authors' papers [7,15,19,20] that were aimed at investigating the free nonlinear oscillations of planar beams of arbitrary slenderness and with arbitrary end constraint in the axial direction, where k_g was used.

In order to focus on the differences between the use of k_m or k_g, and following [7,15,19,20], we consider a linearly elastic constitutive behaviour, i.e.

$$M = EJ\,k_m \quad (\text{"mechanical"model}), \qquad \text{or} \qquad M = EJ\,k_g = \frac{EJ\,k_m}{1+e} \quad (\text{"geometric"model}), \tag{2}$$

EJ being the bending stiffness. Furthermore, planar free oscillations of an initially straight homogenous Timoshenko beam are investigated, where the axial and rotational inertia are taken into account, as well as the shear deformation.

Since in the considered case the nonlinear behaviour is determined by the so-called backbone curve

$$\omega = \omega(a) = \omega_0 + \omega_2 a^2 + ..., \tag{3}$$

giving the natural (circular) frequency ω as a function of the oscillation amplitude a, the comparison is made in terms of ω_2, as ω_0 is the same for both models being the linear frequency.

2. The governing equations for the two models

We consider the beam reported in Fig. 1, and we denote by $W(Z,T)$ and $U(Z,T)$ the axial and the transversal displacements of the beam axis, respectively. Z is the spatial coordinate in the *rest* rectilinear configuration, which ranges from 0 to the length L. T is the physical time. κ is the stiffness of the spring at the right-end of the beam, which allows us to encompass cases from the axially free ($\kappa = 0$) to the axially constrained ($\kappa \to \infty$).

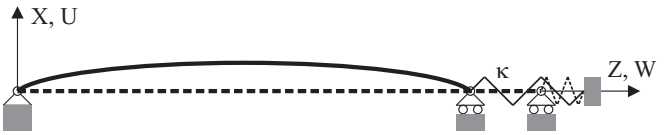

Fig. 1. Current configuration (continuous line) of the initially straight (dashed line) beam with end spring of stiffness κ. U and W are the transversal and axial displacements, respectively.

In [7], based on kinematics, balance and the constitutive behaviour $M = EJ\,k_g$, the following exact PDEs of motion are obtained for the "geometric" model:

$$\begin{aligned}
&\left\{EA[\sqrt{(1+W')^2+U'^2}-1]\frac{1+W'}{\sqrt{(1+W')^2+U'^2}}+GA\left[\theta-\arctan\left(\frac{U'}{1+W'}\right)\right]\frac{U'}{\sqrt{(1+W')^2+U'^2}}\right\}' = \omega^2\rho A\,\ddot{W},\\
&\left\{EA[\sqrt{(1+W')^2+U'^2}-1]\frac{U'}{\sqrt{(1+W')^2+U'^2}}-GA\left[\theta-\arctan\left(\frac{U'}{1+W'}\right)\right]\frac{1+W'}{\sqrt{(1+W')^2+U'^2}}\right\}' = \omega^2\rho A\,\ddot{U}, \quad (4)\\
&\left[EJ\frac{\theta'}{\sqrt{(1+W')^2+U'^2}}\right]'-GA\left[\theta-\arctan\left(\frac{U'}{1+W'}\right)\right]\sqrt{(1+W')^2+U'^2} = \omega^2\rho J\,\ddot{\theta},
\end{aligned}$$

where the time is rescaled as $t = \omega T$ (this is needed to apply the Poincaré-Lindstedt method), the dot means derivative with respect to t and prime derivative with respect to Z. We refer to [7,15] for the definition of the various parameters appearing in (4) and for further details.

Considering the constitutive behaviour $M = EJ\,k_m$ we obtain the "mechanical" model. The first two equations $(4)_1$ and $(4)_2$ do not vary, since they represent the translation dynamic balance equations in the axial and transversal directions and thus are not affected by the curvature (and in fact EJ does not appear in those equations). Equation $(4)_3$, on the other hand, represents the rotational dynamic balance equation, and changes to the simpler expression

$$[EJ\theta']' - GA\left[\theta-\arctan\left(\frac{U'}{1+W'}\right)\right]\sqrt{(1+W')^2+U'^2} = \omega^2\rho J\,\ddot{\theta}. \quad (5)$$

The boundary conditions associated with both models are [7,15]

$$U(0,T)=0, \quad U(L,T)=0, \quad M(0,T)=0, \quad M(L,T)=0, \quad W(0,T)=0, \quad H_o(L,T)+\kappa W(L,T)=0, \quad (6)$$

where H_o is the horizontal (in the Z-direction) internal force.

3. Asymptotic solution

According to the Poincaré-Lindstedt method, the solution is sought after in the form

$$\begin{aligned}
&W(Z,t)=\varepsilon W_1(Z,t)+\varepsilon^2 W_2(Z,t)+\varepsilon^3 W_3(Z,t)+..., \quad && U(Z,t)=\varepsilon U_1(Z,t)+\varepsilon^2 U_2(Z,t)+\varepsilon^3 U_3(Z,t)+...,\\
&\theta(Z,t)=\varepsilon\theta_1(Z,t)+\varepsilon^2\theta_2(Z,t)+\varepsilon^3\theta_3(Z,t)+..., && \omega=\omega_0+\varepsilon\omega_1+\varepsilon^2\omega_2+...,
\end{aligned} \quad (7)$$

where ε is a small parameter that underlines that we are considering moderately large nonlinear oscillations.

Inserting the expressions (7) in the governing equations, and equating to zero the coefficients of ε^n, we get the following sequence of linear problems, which have been solved in [7,15] for the "geometric" model.

3.1. First order solution

The first order terms $U_1(Z,t)$, $W_1(Z,t)$ and $\theta_1(Z,t)$ are given by ($n \in \mathbb{N}$ is the order of the natural frequency)

$$\begin{aligned}
&U_1(Z,t)=U_a\sin(\lambda_{U1}Z)\sin(t), \quad \theta_1(Z,t)=U_a\alpha_1\lambda_{U1}\cos(\lambda_{U1}Z)\sin(t), \quad W_1(Z,t)=0,\\
&\alpha_1=\frac{GA}{GA-\rho J\omega_0^2+EJ\lambda_{U1}^2}, \quad \lambda_{U1}=\frac{n\pi}{L}.
\end{aligned} \quad (8)$$

The hypothesis $W_1 = 0$ has been removed in [19], although it is kept in this work.

The first order (linear) natural frequency is given by

$$\omega_0 = \frac{1}{L^2}\sqrt{\frac{EJ}{\rho A}}\bar{\omega}_0, \quad \bar{\omega}_0 = l\sqrt{\frac{zl^2 + n^2\pi^2(1+z) - \sqrt{z^2l^4 + 2zn^2\pi^2(1+z)l^2 + n^4\pi^4(1-z)^2}}{2}}, \tag{9}$$

where the slenderness of the beam $l = L\sqrt{(A/J)}$ and the dimensional shear stiffness $z = [2(1+\nu)\chi]^{-1}$ (ν is the Poisson coefficient and χ is the shear correction factor, equal to $6/5$ for rectangular cross-section) have been used to obtain

$$EA = \frac{EJ}{L^2}l^2, \quad \rho J = \frac{\rho A L^2}{l^2}, \quad GA = \frac{EJ}{L^2}l^2 z. \tag{10}$$

For following purposes, we also define the dimensionless stiffness of the end spring $\kappa_h = \kappa\frac{L^3}{EJ}$.

For slender beams ($l \to \infty$) we have

$$\bar{\omega}_0 = n^2\pi^2 - \frac{n^4\pi^4}{2}\left(1 + \frac{1}{z}\right)\frac{1}{l^2} + ... \tag{11}$$

The solution described by (8) and (9) corresponds to the linear term, and thus, while being obtained for the "geometric" model, it is valid also for the "mechanical" model.

3.2. Second order solution

The second order solution, *which is valid for both models*, is obtained by means of appropriate solvability conditions of the second order equations, and is given by

$$\begin{aligned}
&U_2(Z,t) = 0, \quad \theta_2(Z,t) = 0, \quad W_2(Z,t) = W_{2a}(Z) + W_{2b}(Z)\cos(2t), \quad \omega_1 = 0,\\
&\frac{W_{2a}(Z)}{U_a^2} = -\frac{\lambda_{U1}}{16}\frac{EA + 2GA(\alpha_1 - 1)}{EA}\sin(2\lambda_{U1}Z) + \frac{c_1}{L}\frac{Z}{L}, \quad c_1 = -\frac{\frac{1}{8} + \frac{GA}{4EA}(\alpha_1 - 1)}{1 + \frac{\kappa L}{EA}}L^2\lambda_{U1}^2,\\
&\frac{W_{2b}(Z)}{U_a^2} = \frac{\lambda_{U1}^3}{16}\frac{EA + 2GA(\alpha_1 - 1)}{EA\lambda_{U1}^2 - \rho A\omega_0^2}\sin(2\lambda_{U1}Z) + \frac{c_2}{L}\sin\left(\frac{2\omega_0\sqrt{\rho A}}{\sqrt{EA}}Z\right),\\
&c_2 = \frac{[EA + 2GA(\alpha_1 - 1)](2\rho A\omega_0^2 - EA\lambda_{U1}^2)}{2\omega_0\sqrt{\rho A}\sqrt{EA}\cos\left(\frac{2\omega_0\sqrt{\rho A}}{\sqrt{EA}}L\right) + \kappa L\sin\left(\frac{2\omega_0\sqrt{\rho A}}{\sqrt{EA}}L\right)}\frac{L}{8\left(\frac{\rho A\omega_0^2}{\lambda_{U1}^2} - EA\right)}.
\end{aligned} \tag{12}$$

3.3. Third order solution

The solvability condition of the third order equations provides the backbone nonlinear correction term

$$\omega_2 = U_a^2\left[c_1\frac{\omega_{2a}}{\omega_{2d}} + c_2\sin\left(\frac{2L\omega_0\sqrt{\rho A}}{\sqrt{EA}}\right)\frac{\omega_{2b}}{\omega_{2d}} + \frac{\omega_{2c}}{\omega_{2d}}\right] = \left(\frac{U_a}{L}\right)^2\frac{1}{L^2}\sqrt{\frac{EJ}{\rho A}}\bar{\omega}_2, \tag{13}$$

where $\bar{\omega}_2$ is a dimensionless quantity, implicitly defined by (13), that depends on l (slenderness), z (shear stiffness) and κ_h (spring stiffness) (see [15]).

Equations $(9)_1$ and $(13)_2$ allow us to rewrite (3) in the form

$$\omega = \frac{1}{L^2}\sqrt{\frac{EJ}{\rho A}}\left[\bar{\omega}_0 + \left(\frac{\varepsilon U_a}{L}\right)^2\bar{\omega}_2 + ...\right], \tag{14}$$

where $a = \varepsilon U_a/L$ is the dimensionless amplitude of the (first order) oscillations (see (7) and (8)).

3.3.1. Geometric model

For the "geometric" model the parameters ω_{2a}, ω_{2b}, ω_{2c} and ω_{2d} are[7,15]:

$$\begin{aligned}
&\omega_{2a} = 32EA\pi^2n^2(EA\pi^2n^2 - \omega_0^2L^2\rho A)[EAL^2 - \mathbf{EJ}\pi^2n^2\alpha_1^2 + GAL^2(\alpha_1^2 - 1)],\\
&\omega_{2b} = 16EA\pi^2n^2GAL^2(\alpha_1^2 - 1)(2\rho A\omega_0^2L^2 - EA\pi^2n^2) + 16(EA)^2\pi^2n^2(\mathbf{EJ}\alpha_1^2\pi^4n^4 - EA\pi^2n^2L^2 + 2\rho A\omega_0^2L^4),\\
&\omega_{2c} = 6\pi^6n^6L^2(EA)^3 - \pi^4n^4(EA)^2[-6\pi^2n^2L^2(\alpha_1^2 - 1)GA + 6\pi^4n^4\alpha_1^2\mathbf{EJ} + 7\rho A\omega_0^2L^4] +\\
&\quad + EA\{\pi^6n^6\alpha_1^2[-6\pi^2n^2(\alpha_1 - 1)GA + 5L^2\rho A\omega_0^2]\mathbf{EJ} - \pi^4n^4L^2GA(\alpha_1 - 1)[6n^2\pi^2(\alpha_1^2 - 1)GA +\\
&\quad + \omega_0^2L^2\rho A(7\alpha_1 + 9)]\} + 4\rho A(\alpha_1 - 1)L^2GA\pi^4n^4\omega_0^2[(\alpha_1^2 - 1)L^2GA + n^2\pi^2\alpha_1^2\mathbf{EJ}],\\
&\omega_{2d} = 64EAL^4\omega_0(EA\pi^2n^2 - \omega_0^2L^2\rho A)(\rho AL^2 + \pi^2n^2\alpha_1^2\rho J).
\end{aligned} \tag{15}$$

For slender beams ($l \to \infty$) we have

$$\begin{aligned}
&\bar{\omega}_2^{geom} = n^2\pi^2\left(\frac{3}{32}\kappa_h + \frac{15}{64}n^2\pi^2 - \frac{1}{24}n^4\pi^4\right) + \frac{n^2\pi^2}{l^2}\left[-\frac{3}{32}\kappa_h^2 + n^2\pi^2\left(\frac{1}{12}n^2\pi^2 - \frac{\mathbf{37}}{64}\right)\kappa_h\right.\\
&\left. + n^4\pi^4\left(-\frac{1}{15}n^4\pi^4 + \frac{\mathbf{17}}{48}n^2\pi^2 - \frac{\mathbf{153}}{128}\right) + \frac{n^2\pi^2}{z}\left(\frac{1}{48}n^4\pi^4 - \frac{15}{128}n^2\pi^2 + \frac{3}{64}\kappa_h\right)\right] + ...
\end{aligned} \tag{16}$$

3.3.2. Mechanical model

For the "mechanical" model the parameters ω_{2a}, ω_{2b}, ω_{2c} and ω_{2d} are:

$$\begin{aligned}
&\omega_{2a} = 32EA\pi^2n^2(EA\pi^2n^2 - \omega_0^2L^2\rho A)[EAL^2 + GAL^2(\alpha_1^2 - 1)],\\
&\omega_{2b} = 16EA\pi^2n^2GAL^2(\alpha_1^2 - 1)(2\rho A\omega_0^2L^2 - EA\pi^2n^2) + 16(EA)^2\pi^2n^2(-EA\pi^2n^2L^2 + 2\rho A\omega_0^2L^4),\\
&\omega_{2c} = 6\pi^6n^6L^2(EA)^3 - \pi^4n^4(EA)^2[-6\pi^2n^2L^2(\alpha_1^2 - 1)GA + 7\rho A\omega_0^2L^4] +\\
&\quad + EA\{-\pi^4n^4L^2GA(\alpha_1 - 1)[6n^2\pi^2(\alpha_1^2 - 1)GA +\\
&\quad + \omega_0^2L^2\rho A(7\alpha_1 + 9)]\} + 4\rho A(\alpha_1 - 1)L^2GA\pi^4n^4\omega_0^2[(\alpha_1^2 - 1)L^2GA],\\
&\omega_{2d} = 64EAL^4\omega_0(EA\pi^2n^2 - \omega_0^2L^2\rho A)(\rho AL^2 + \pi^2n^2\alpha_1^2\rho J).
\end{aligned} \tag{17}$$

For slender beams ($l \to \infty$) we have

$$\begin{aligned}
&\bar{\omega}_2^{mech} = n^2\pi^2\left(\frac{3}{32}\kappa_h + \frac{15}{64}n^2\pi^2 - \frac{1}{24}n^4\pi^4\right) + \frac{n^2\pi^2}{l^2}\left[-\frac{3}{32}\kappa_h^2 + n^2\pi^2\left(\frac{1}{12}n^2\pi^2 - \frac{\mathbf{31}}{64}\right)\kappa_h\right.\\
&\left. + n^4\pi^4\left(-\frac{1}{15}n^4\pi^4 + \frac{\mathbf{15}}{48}n^2\pi^2 - \frac{\mathbf{139}}{128}\right) + \frac{n^2\pi^2}{z}\left(\frac{1}{48}n^4\pi^4 - \frac{15}{128}n^2\pi^2 + \frac{3}{64}\kappa_h\right)\right] + ...
\end{aligned} \tag{18}$$

By comparing expressions (15) and (17) we see that the coefficients for the "mechanical" model are obtained by setting $EJ = 0$ in the coefficients of the "geometric" model. ω_{2d} is the same for both models.

On the contrary, the comparison of (16) and (18) shows that there are very minor differences (the three numbers reported in bold in the formulas) in the nonlinear correction coefficient obtained with the two models. Furthermore, we note that the dominating term in the two asymptotic expansions is the same, so that we can conclude that for slender beams the two models coincide, and for non-slender beams the differences should be limited.

4. Comparison for different slenderness and boundary condition

The detailed study of the backbone curve has been done in[7,15,19,20] for the "geometric" model. Here, instead of performing the same analysis for the "mechanical" model, we prefer to compare ω_2^{mech} with ω_2^{geom} to better highlight the differences between the two models.

The ratio $\omega_2^{mech}/\omega_2^{geom}$ is reported in Fig. 2 as a function of κ_h for the three fixed values of l used in[20] (so that in this case we also have a numerical confirmation of the analytical results). The ratio is approximately constant and greater than 1 (consistent with the stiffer mechanical model), apart from the critical points where the ratio is 0 (for $\omega_2^{mech} = 0$) or it goes to infinity (for $\omega_2^{geom} = 0$), which however are close to each other (for example, for the case of Fig. 2a we have $\kappa_h = 21.8521$ vs $\kappa_h = 21.7491$, respectively). The conclusion is that κ_h affects the results only slightly.

Apart from the neighborhood of the critical points, which is very small and thus unimportant from a practical point of view, we note that ω_2^{mech} and ω_2^{geom} have the same sign, so that the two models prescribe the same hardening/softening behaviour, and thus are consistent.

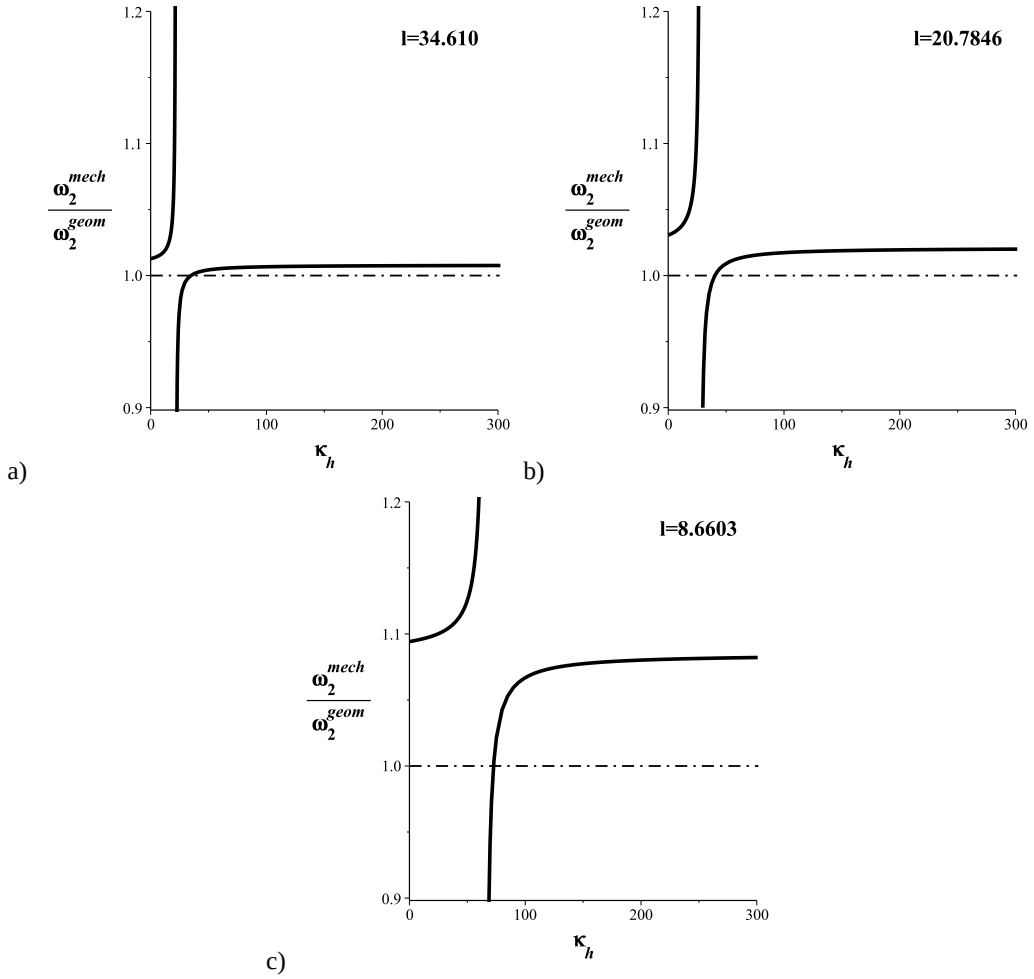

Fig. 2. The ratios $\omega_2^{mech}/\omega_2^{geom}$ as function of κ_h for different values of l. $n = 1$ and $z = 0.3205$.

The (almost constant) value of the ratio increases by decreasing l, with the major difference occurring for the thicker beam, where however the difference is only about 8%. For slender beams, on the other hand, the difference is negligible from a quantitative point of view, and vanishes for very slender beams.

To better appreciate the effect of the slenderness, we start to compute the asymptotic expansion for $l \to \infty$:

$$\frac{\omega_2^{mech}}{\omega_2^{geom}} = 1 + \frac{n^2\pi^2}{l^2}\frac{8n^4\pi^4 - 21n^2\pi^2 - 18\kappa_h}{8n^4\pi^4 - 45n^2\pi^2 - 18\kappa_h} + ..., \tag{19}$$

which confirms that the two models are substantially identical for slender beams.

We report in Fig. 3a the ratio as a function of l for the hinged-supported ($\kappa_h = 0$) and the hinged-hinged ($\kappa_h \to \infty$) cases. The two curves are very close to each other, and the curves for all other values of κ_h (apart from the critical points) are in-between, confirming the low effect of κ_h highlighted above.

The two curves have a maximum of 13.1% and 13.6%, at $l = 4.520$ and $l = 4.252$, respectively. These numbers confirm also from a quantitative point of view the closeness of the two curves, and further show that the largest difference between the two models is about 13% and occurs for very low slenderness, at the limit of practical application. After the maximum the curves are decreasing and rapidly approach 1, confirming that even for not so slender beams the outcomes of two models are identical (for example, the difference of 1% is obtained yet for $l \simeq 40$).

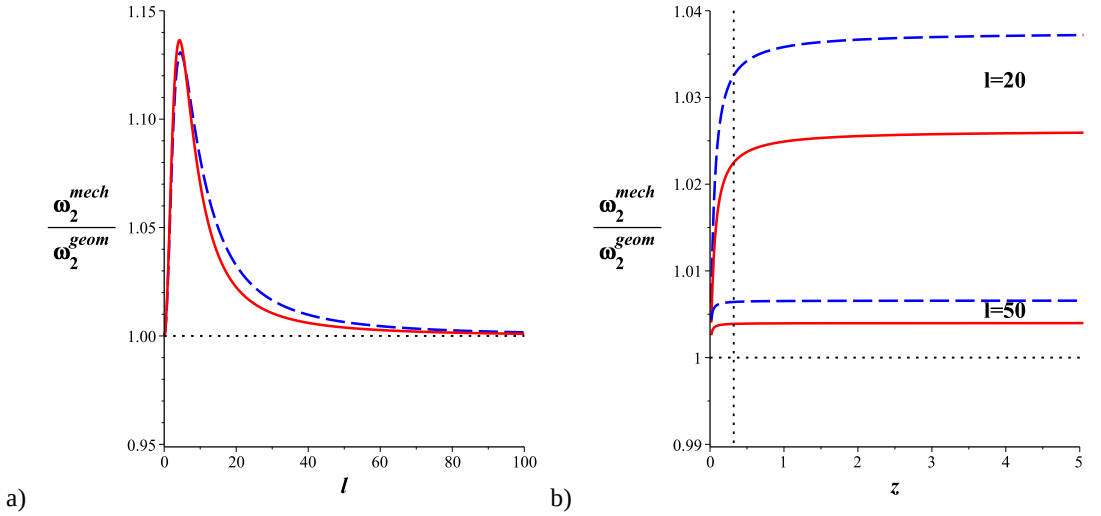

Fig. 3. The ratios $\omega_2^{mech}/\omega_2^{geom}$ for $n = 1$. a) as function of l for $\kappa_h = 0$ (dash blue line) and $\kappa_h \to \infty$ (solid red line), $z = 0.3205$; b) as a function of z for $\kappa_h = 0$ (dash blue line) and $\kappa_h \to \infty$ (solid red line), and two different values of l (the vertical line corresponds to $z = 0.3205$).

Figure 3b, on the other hand, shows the substantial independence of the ratio on the shear stiffness coefficient z, apart from the sharp decrease occurring for highly shear deformable beam elements where the anyway lower value of the geometric curvature with respect to the mechanical one plays a role.

5. Softening/hardening transition

It has been shown in [7,15,19,20] that the main nonlinear dynamical feature of the considered mechanical system is that it can change its nonlinear behavior from softening ($\omega_2 < 0$) to hardening ($\omega_2 > 0$) by varying the system parameters. This occurs when $\omega_2 = 0$, which is the simplest case, but also when $\omega_2 \to \infty$. Let us start with this latter condition, which happens when the denominators of ω_2 vanish. Since ω_{2d} is always different from zero [7,15], this occurs when the denominator of c_2 (see (12)) vanishes, namely

$$\kappa = -\frac{2\omega_0\sqrt{\rho A}\sqrt{EA}}{L}\frac{1}{\tan\left(\frac{2\omega_0\sqrt{\rho A}}{\sqrt{EA}}L\right)} \quad \to \quad \kappa_h = -\frac{2l\bar{\omega}_0}{\tan\left(\frac{2\bar{\omega}_0}{l}\right)}. \tag{20}$$

It is worth to remark that *this condition is the same for both models.*

The other transition condition $\omega_2 = 0$ provides two (one per model) second order algebraic equations in the unknown κ_h, which can be easily solved. The transitions loci are reported in Fig. 4, which for the "geometric" model is the same of Fig. 12c of [15]. The differences between the two models are very minor, and can be appreciated only on the enlargement of Fig. 4b.

6. Conclusions

The nonlinear oscillations of a Timoshenko beam with arbitrary slenderness and arbitrary boundary condition in the axial direction have been investigated. Axial and rotational inertia have been considered, and the solution is obtained by means of the Poincaré-Lindstedt asymptotic method.

Attention is focused on the different definition of the curvature, as the derivative with respect to the deformed length ("geometric") or with respect to the undeformed length ("mechanical"). The two models are compared to each other. Since the difference appears only in the nonlinear regime, the comparison is made in term of the nonlinear correction coefficient of the backbone curve.

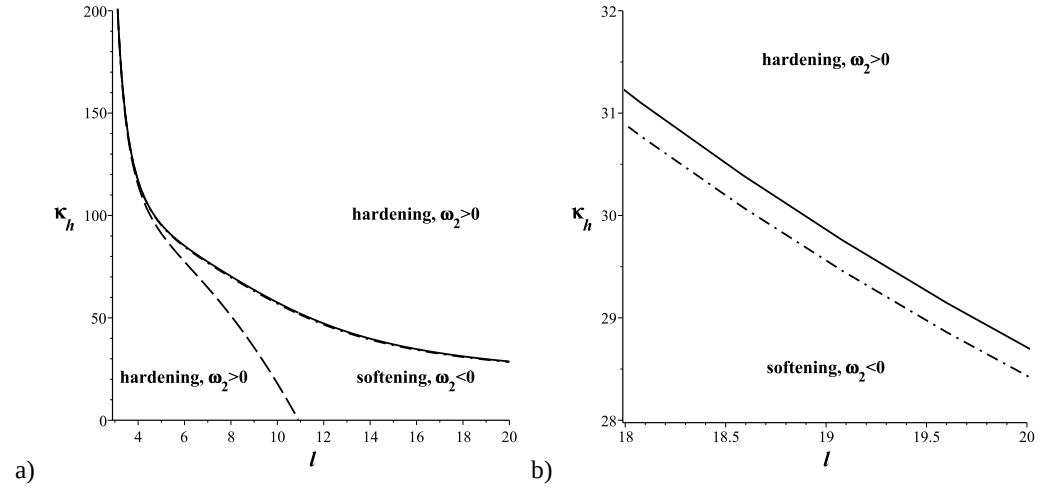

Fig. 4. The solution of $\omega_2 = 0$ (solid line) for the "geometric" model, of $\omega_2 = 0$ (dashdot line) for the "mechanical" model, and of $\omega_2 \to \infty$ (dashed line) in the (l, κ_h) plane. $n = 1$ and $z = 0.3205$.

It has been shown that the two models give the same nonlinear behaviour for slender beams, while some difference, up to about 13%, can be observed for thick beams. Furthermore, the stiffness of the end spring does not influence the differences between the two models.

The general conclusion is that using, in moderately large nonlinear free oscillations, the "geometric" or the "mechanical" curvature does not affect the results that much, especially for slender beams.

References

1. Villaggio P. *Mathematical Models for Elastic Structures*. Pisa: Cambridge University Press; 1997. ISBN: 0-521-57324.
2. Antman SS. *Nonlinear Problems of Elasticity*. Second edition. New York: Springer; 2005. ISBN 0-387-20880-1.
3. Trabucho L, Viano JM. Mathematical modelling of rods. In: Ciarlet PG, Lions JL, editors. *Handbook of Numerical Analysis*, Vol. IV. North-Holland; 1996.
4. Ciarlet PG. *Mathematical Elasticity, Vol. II: Theory of Plates*. Amsterdam: North-Holland; 1997. ISBN: 0-444-82570-3.
5. Podio-Guidugli P. An exact derivation of the thin plate equation. *J Elasticity* 1989; **22**: 121-133.
6. Nayfeh AH, Pai PF. *Linear and Nonlinear Structural Mechanics*. New York: Wiley; 2004. ISBN: 978-0-471-59356-0.
7. Lenci S, Rega G. Nonlinear free vibrations of planar elastic beams: A unified treatment of geometrical and mechanical effects. *Procedia IUTAM, IUTAM Symposium Analytical Methods in Nonlinear Dynamics* 2016; **19**: 35-42.
8. Lacarbonara W. *Nonlinear Structural Mechanics*. New York: Springer; 2013. ISBN: 978-1-4419-1276-3.
9. Luongo A, Zulli D. *Mathematical Models of Beams and Cables*. New York: Wiley-ISTE; 2013. ISBN: 978-1-84821-421-7.
10. Gerstmayr J, Irschik H. On the correct representation of bending and axial deformation in the absolute nodal coordinate formulation with an elastic line approach. *J Sound Vibr* 2008; **318**: 461-487.
11. Géradin M, Cardona A. *Flexible Multibody Dynamics. A Finite Element Approach*. New York: Wiley; 2001. ISBN: 978-0-471-48990-0.
12. Simo JC, Vu-Quoc L. A geometrically-exact beam model incorporating shear and torsion warping deformation. *Int. J. Solids Struct* 1991; **27**: 371-393.
13. Hodges DH. Proper definition of curvature in nonlinear beam kinematics. *AIAA J.* 1984; **22**; 1825-1827.
14. Cao DQ, Tucker RW. Nonlinear dynamics of elastic rods using the Cosserat theory: Modelling and simulation. *Int J Solids Struct* 2008; **45**: 460-477.
15. Lenci S, Clementi F, Rega G. A comprehensive analysis of hardening/softening behaviour of shearable planar beams with whatever axial boundary constraint. *Meccanica* 2016. In press. DOI: 10.1007/s11012-016-0374-6.
16. Magrab EB. *Vibrations of Elastic Systems with Applications to MEMS and NEMS*. New York: Springer; 2012. ISBN 978-94-007-2672-7.
17. Babilio E. Dynamics of an axially functionally graded beam under axial load. *Eur Phys J Special Topics* 2013; **222**: 1519-1539.
18. Berzeri M, Shabana AA. Development of simple models for the elastic forces in the absolute nodal co-ordinate formulation. *J Sound Vibr* 2000; **235**: 539-565.
19. Lenci S, Rega G. Axial-transversal coupling in the free nonlinear vibrations of Timoshenko beams with arbitrary slenderness and axial boundary conditions. *Proc Royal Soc A* 2016; **472**; 20160057.
20. Clementi F, Lenci S, Rega G. Cross-checking asymptotics and numerics in the hardening/softening behavior of Timoshenko beams with axial end spring and variable slenderness. *Arch Appl Mech* 2016. In press. DOI: 10.1007/s00419-016-1159-z